J Mater Sci (2007) 42:2591–2597
DOI 10.1007/s10853-006-1337-4

The study of tri-phasic interactions in nano-hydroxyapatite/konjac glucomannan/chitosan composite

Zhou Gang · Li Yubao · Zhang Li · Li Hong · Wang Mingbo · Cheng Lin · Wang Yuanyuan · Wang Huanan · Shi Pujiang

Received: 26 November 2005 / Accepted: 9 March 2006 / Published online: 2 January 2007

Abstract The interactions among the three phases of nano-hydroxyapatite (n-HA), Konjac glucomannan (KGM) and Chitosan (CS) in n-HA/KGM/CS composite were investigated using TEM, IR, XRD, XPS and TGA methods. The crystalline structure of n-HA was studied by means of Rietveld method. A series of structure parameters, such as, cell lattice parameters (*a* or *c*), bonding lengths and a numerical index of distortion for PO_4 tetrahedron, were calculated by Newton–Raphson calculating method to characterize the crystalline structure of HA at atom level. The results showed that n-HA was mainly linked with KGM and CS by hydrogen bonding between OH^-–PO_4^{3-} of n-HA and –C=O, –NH of KGM-CS copolymer, and there was a stable interface formed between the three phases in the composite. Besides, orientation of this hydrogen bonding resulted in the decrease of the relative crystallization degree of KGM-CS copolymer.

Introduction

Bone repair or regeneration is a common and complicated clinical problem in orthopaedic surgery. Until now, some biomaterials have been developed and their clinical testing has been done. Hydroxyapatite (HA), being able to form a direct chemical bonding with surrounding tissues, has been proposed as substitute for defective bones or teeth due to its good biocompatibility, bioactivity and osteoconductivity [1–4].

Recently, great attentions have been focused on the composites based on HA reinforced polymeric matrix. Natural and biodegradable polymers are considered as ''interesting'' alternatives for the development of new biodegradable composites.

Polysaccharides are a class of biopolymers composed of simple sugar monomers. Chitosan (CS) is a biodegradable and semicrystalline polysaccharide obtained from N-deacetylation of chitin, which is harvested from the exoskeleton of marine crustaceans [5–8]. Konjac glucomannan (KGM) is water-soluble and non-ionic glucomannan with a high molecular weight found in tubers of the *Amorphophallus konjac* plant [9, 10]. CS and KGM schematic structures are shown in Fig. 1. It is noted that facilitating hydrogen-bonding formation of excessive hydroxyl groups in KGM with other polymers results in gelatin or enhances miscibility in binary system of KGM with other polymers [11].

We have prepared a composite using n-HA, KGM and CS by co-precipitation method to facilitate particulate immobilization and accelerate the biodegradation of the new biomaterial. In this paper, TEM, IR, XRD, XPS, TGA and Rietveld method are used to clarify the interactions among n-HA, KGM and CS in the composite, and determine the effects of these interactions on the crystallization behavior of KGM-CS copolymer.

Z. Gang · L. Yubao (✉) · Z. Li · L. Hong · W. Mingbo · C. Lin · W. Yuanyuan · W. Huanan · S. Pujiang
Research Center for Nano-Biomaterials, Analytical & Testing Center, Sichuan University, Chengdu 610064, People's Republic of China
e-mail: nic7504@scu.edu.cn

Z. Gang · L. Hong · W. Mingbo · C. Lin
College of Chemistry, Sichuan University, Chengdu 610064, People's Republic of China

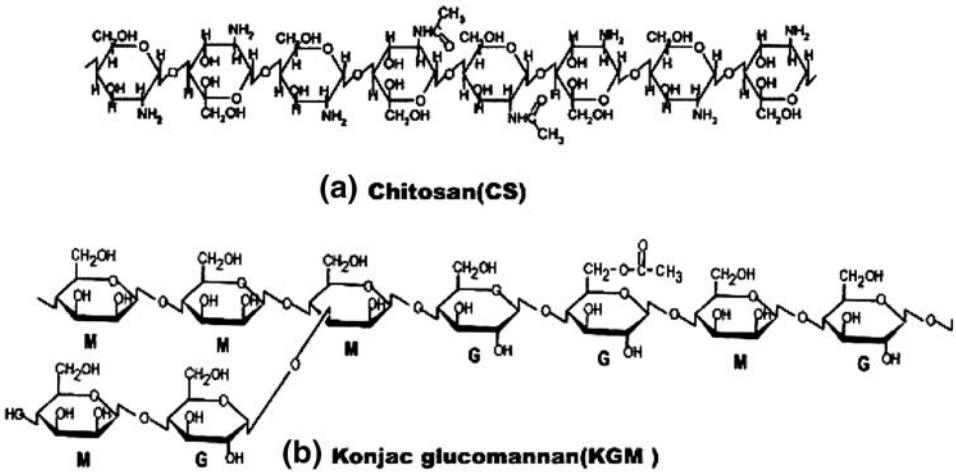

Fig. 1 Schematic of polysaccharides molecular structure: CS (**a**), KGM (**b**) [12, 13]

Materials and methods

Materials

Eighty-mesh CS powder was purchased from Haidebei Bioengineering Co. Ltd., Jinan, China. Eighty-mesh KGM powder was purchased from Baishilong Technology Co. Ltd., Chengdu, China. Calcium hydroxide, phosphoric acid and all other reagents used here were analytical grade. Calcium hydroxide was screened through a 200-mesh sieve before used.

Preparation of the materials

The composites were synthesized by the following procedure. First, KGM powders were dissolved into a 10 wt% H_3PO_4 aqueous solution, noted as A solution. Then CS powders were added into A solution with stirring for 1 h to get a semi-transparent solution, noted as B solution. The starting content of these reagents was scaled according to the final n-HA/KGM/CS weight ratio of 70/15/15. The mixed B solution was then dropped slowly into the 8 wt% $Ca(OH)_2$ aqueous solution with vigorously stirring and the pH was adjusted to 10 by adding concentrated $NH_3 \cdot H_2O$. The dropping speed was around 4 ml min^{-1} and the reaction was carried out in ambient condition. The stirring speed was adjusted to 1,000 rpm. After titration, the stirring was kept for 24 h, and then the obtained slurry was aged for another 24 h. Finally, the precipitate was filtered and washed with de-ionized water and dried in a vacuum oven at 80 °C. n-HA was synthesized by $Ca(OH)_2$ and H_3PO_4 [14] at the same ambient as that of composite synthesized.

Characterization

TEM

The microstructures of n-HA and n-HA/KGM/CS composites powders were observed with a transmission electron microscope (TEM, JME-100CX).

XPS

X-ray photo-electronic spectroscopy (XPS, XSAM 800) was applied to analyze the surface area of n-HA/KGM/CS composite powders.

FT-IR

Chemical analysis of the composites was carried out by a Fourier transform infrared (FT-IR) spectrophotometer (Thermo Nicolet 170SX FT-IR Spectrometer) in the range from 4000 cm^{-1} to 400 cm^{-1} at 2 cm^{-1} resolution averaging 100 scans.

X-ray diffraction

X-ray diffraction (XRD) was used to determine the structure of materials. XRD measurements were performed with a Philips X' Pert MPD XRD analyzer (CuKα). The samples were measured in the 2θ range from 5° to 60°.

Rietveld analysis

The crystal structures of HA were refined using the Rietveld method. Rietveld refinement was performed using the Cerius 2 program package. A numerical index (dimensionless) of the overall distortion (D_{ind}) of

the structure may be calculated from the PO_4 tetrahedron. The numerical index (D_{ind}) represents the deviation of the PO_4 tetrahedron from an optimal configuration and is derived from:

$$D_{ind} = \sum (\theta_i - 109.170)^2/6 \text{ (Å)}$$

with θ = angle O–P–O [15, 16].

TGA

The thermogravimetric analysis (TGA) of the composites was studied on 50 mg of powder samples using a TG analyzer (Exstar 6000) and measurements were recorded from 25°C to 800°C at 10°C min^{-1} heating rate under a nitrogen atmosphere.

Results and discussion

TEM observation

TEM photograph of n-HA/KGM/CS composite is shown in Fig. 2. The composite powders show a slimly shuttle-like morphology with an average size of about 90 ± 5 nm in length and 15 ± 5 nm in width. Meanwhile, these n-HA crystals can disperse uniformly in the polymer matrix and display a relatively uniform morphology. Besides the inorganic particles were added into the copolymer matrix, these powders could combine closely with the organic matrix.

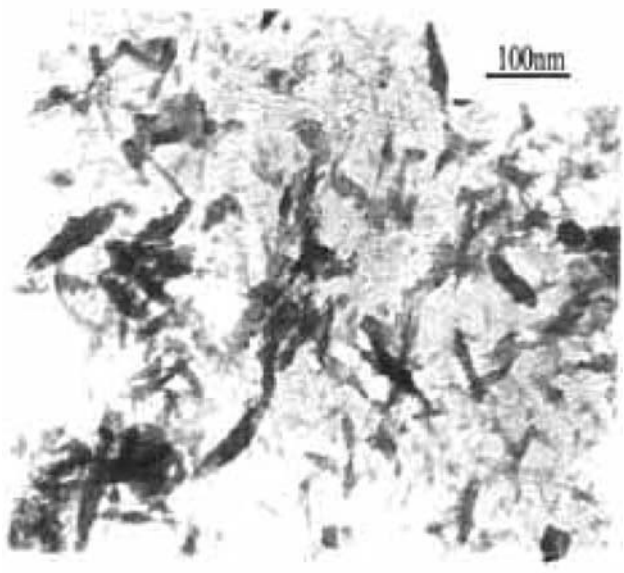

Fig. 2 TEM spectrum of n-HA/KGM/CS composite powders

XPS analysis

Figure 3 is the XPS curves of n-HA and n-HA/KGM/CS composite. The binding energy of Ca, P and O atoms has some differences between n-HA (Ca: 350.5 and 345.5; O: 530.2; P: 132.5 eV) and the composite (Ca: 352.1 and 347.4; O: 531.2; P: 133.4 eV). The values of atoms in the composite are higher than those of n-HA. This means that the binding energy of Ca, O and P increase in the composite. This means that there would be some interaction or chemical bonding formed between three phases. This may be caused by the affinity between Ca^{2+}, –OH, PO_4^{3-} in n-HA and –OH, –CONH groups in KGM-CS copolymer.

IR analysis

Figure 4a, b, c and d are IR patterns of the n-HA, KGM, CS and n-HA/KGM/CS composite, respectively. Several changes of characteristic groups can be noted in the Table 1 and the values indicate that: (1) the stretching vibration bands of $–CH_2–$ and –CH– in KGM and CS are moved to higher wavenumber, which suggests that the n-HA particles might enter into the networks of KGM-CS fibrils and disturb the arrangement of polymer in the composite. (2) Only $\sigma_{3\text{-}2}$(1,031 cm^{-1}) and $\sigma_{4\text{-}2}$(563 cm^{-1}) of PO_4^{3-} groups shift to 1,029 cm^{-1} and 562 cm^{-1}, respectively, and the other bands of PO_4^{3-} are still in the original sites. It implies that the

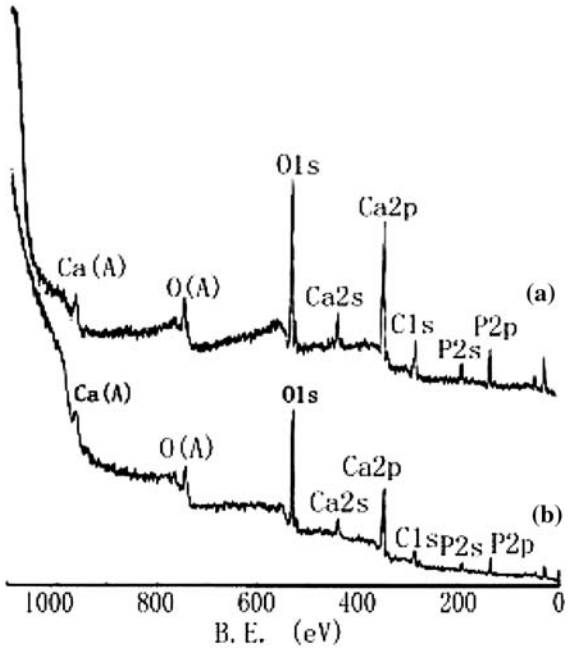

Fig. 3 XPS curves of n-HA/KGM/CS composite (a) and n-HA (b)

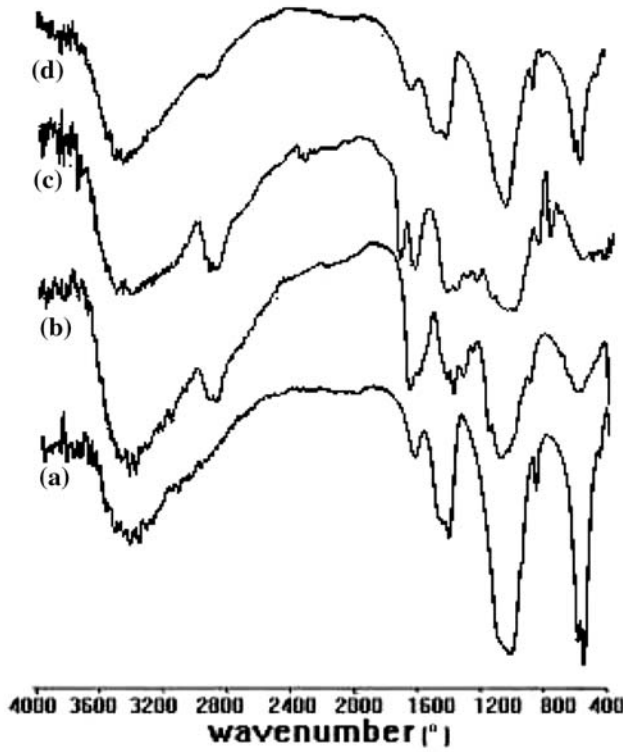

Fig. 4 IR spectra of n-HA (a), CS (b), KGM (c) and n-HA/KGM/CS composite (d)

hydrogen bonding may be formed between the P–O and –N–H of the CS. (3) Two different –C=O stretching vibration bands exist in pure KGM, that is, free –C=O stretching vibration band (1,734 cm^{-1}) and hydrogen bonded –C=O stretching with –OH group band (1,644 cm^{-1}). However, the two bands are overlapped at 1,644 cm^{-1} in the composite, which indicates that hydrogen bonding is formed between –OH and –C=O stretching vibration after mixed. When –C=O reacts with –OH, the –OH belonging to the more electronegative group that attract electrons strongly, the symmetrical electron distributes on the one hand, shown in Fig. 5, which results in the changes of wavenumber. Meanwhile, the characteristic banding of amide I carbonyl stretching in CS shift to lower wavenumber, which is attributed to the hydrogen bonding between the –NH, –C=O groups of KGM-CS and –OH of n-HA. (4) The vibration frequency of OH^- of n-HA in the composite is lower than that of pure n-HA due to the hydrogen bonding between n-HA and KGM-CS, which results in the decrease of the vibration frequency of –OH.

XRD analysis

Figure 6 shows diffraction patterns of n-HA, KGM, CS and n-HA/KGM/CS composite.

According to Bragg formulation [17]

$$2d \sin\theta = \lambda$$

where d is crystal layer spacing, $\theta(^\circ)$ is the angle of incidence and λ is the X-ray wavelength. From Table 2, $d_{(002)}$ = 0.0126 Å, and the θ shifts to smaller angle in the composite, while $d_{(300)}$ = 0.007 Å, in which the θ shifts to the other side. This indicated that the crystal faces of (002) and (300) preferentially orientated parallel to the surfaces of matrix after compounded. The value of change is shown to cause a decrease in *a*-axis and increase the cell in the *c* direction, which endows the structure of n-HA with stability in the composite. From Table 2, it shows that the crystal layer spacing of KGM-CS copolymer phase becomes larger. The changes may be suggested that, when n-HA and KGM-CS copolymer co-precipitated from the solution, n-HA could ''insert'' into copolymer phase and form hydrogen bonding between them. Then, the steric effects and the orientation of hydrogen bonding would enlarge the layer spacing of organic phase. Meanwhile, they lead to the diffraction peaks becoming weaker and wider, which are shown in Fig. 6d.

Table 1 The vibration frequency changes of characteristic groups of n-HA, KGM, CS and and n-HA/KGM/CS composite

	Characteristic group	n-HA (cm^{-1})	CS (cm^{-1})	KGM (cm^{-1})	Comp. (cm^{-1})
HA	–OH	3,571			3,562
		633			623
	$-PO_4^{3-}$	1,094			1,094
		603			603
		1,031			1,029
		563			562
CS	–C=O stretching vibration		1,655		1,643
	$-CH_2$-stretching vibration		2,917		2,987
	–CH- stretching vibration		2,877		2,937
KGM	–C=O stretching vibration			1,734	1,643
				1,644	1,643
	$-CH_2$-stretching vibration			2,921	2,987
	–CH-stretching vibration			2,876	2,937

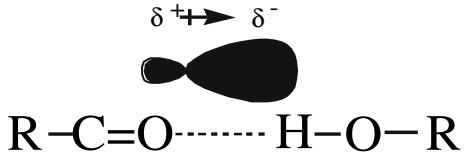

Fig. 5 Schematic of the bonding continuum of two ions

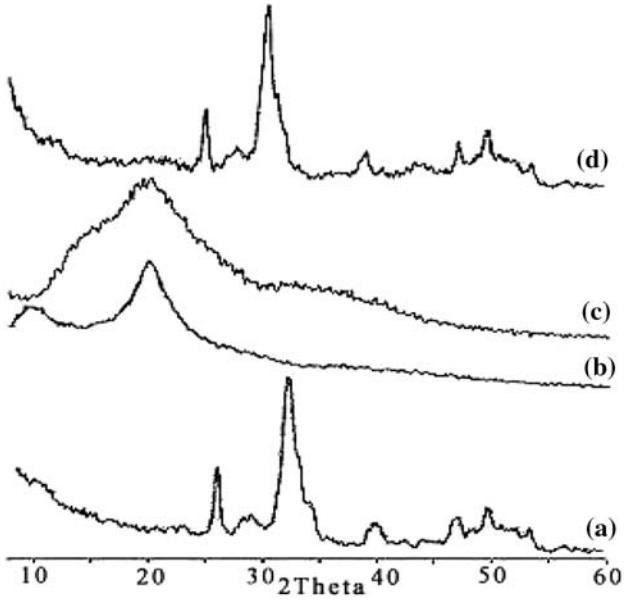

Fig. 6 XRD patterns of n-HA (a), CS (b), KGM (c) and n-HA/KGM/CS composite (d)

The characteristic peaks for n-HA are detected in the spectrum, as shown in Fig. 6a. However, the broadening diffraction peaks indirectly prove that the synthetic n-HA is poor crystalline. In Fig. 6b, two main diffraction peaks of CS at $2\theta = 10.1°$ and 19.8° are observed. Figure 6c is the XRD pattern of pure KGM, which belongs to amorphous crystal, the relatively specific diffraction peak of KGM can be seen at $2\theta = 20°$. CS is usually crystalline due to strong intermolecular interaction between CS chains through intermolecular hydrogen bonding [18]. The interaction of CS chains with KGM, as revealed by FT-IR, would weaken the intermolecular interaction between CS chains and thus decrease its crystalline degree, which were well reflected by the decrease in the diffraction intensity of CS. Meanwhile, the steric effect of KGM breaks the arrangement of the CS linkages, which also made the crystallinity of CS and KGM decrease sharply. Besides, with the introduction of n-HA, it affects the crystallizing behavior of KGM-CS copolymer. According to IR analysis, there is new and strong bonding formed between n-HA and CS-KGM copolymer in the composite. Thus, n-HA can interpenetrate into copolymer network formed between KGM and CS, and disturb the perfect arrangement of KGM and CS, and thus decrease the intensity of organic phases sharply.

Rietveld analysis

Rietveld method is widely used in inorganic material and ceramic researches [19]. Table 3 shows that: (1) the value of *c*-axis increases from 0.6836 nm to 0.6849 nm, while the value decreases from 0.9359 nm to 0.9348 nm in *a*-axis, which means the cell structure changes greatly after compounded; (2) the calculating density of X-ray diffraction decreases, meaning the atoms of cell arrange closely, which is assumed to the strong interaction between n-HA and KGM-CS copolymer. (3) Bonding lengths and distortion index of PO_4 explain the crystal structure of HA at atom level. Hydrogen bonding may be formed between the –OH of n-HA and –C=O of KGM-CS copolymer, or coordinate bonding may be formed between Ca^{2+} and –NH, which result in decreasing the distance of Ca1–O3. Meanwhile, the regularity of PO_4 tetrahedron is worse and distortion index (D_{ind}) of PO_4 tetrahedron increases, which may attribute to hydrogen bonding formed between O of PO_4 and H of –NH. This interaction is the key factor cause to reduce of the symmetry to the non-centrosymmetric space group.

Table 2 Comparative crystallographic properties of n-HA, KGM, CS and n-HA/KGM/CS composite

n-HA	2θ			26.0	31.8	33.2	46.8	49.6
	d(Å)			3.4241	3.1617	2.6952	1.9395	1.8364
	hkl			002	102	300	211	222
CS	2θ (°)	10.8	20.1					
	d(Å)	8.1847	4.4139					
KGM	2θ (°)		20.7					
	d(Å)		4.2873					
Composite	2θ (°)	9.9	19.8	25.9	32.1	33.3	46.8	49.6
	d(Å)	8.9267	4.4800	3.4371	2.2860	2.6873	1.9395	1.8364

Table 3 Result of Riteveld refinements and the related calculation

		Synthesized n-HA	n-HA in composite
Lattice parameter(nm)	*a*	0.9359	0.9348
	c	0.6836	0.6849
Calculating density ($g\ cm^{-3}$)		3.3284	3.2897
P–O1 (nm)		0.1494	0.1502
P–O2 (nm)		0.1507	0.1509
P–O3 (nm)		0.1533	0.1533
P–O4 (nm)		0.1533	0.1533
Ca1–O3 (nm)		0.2988	0.2991
Distortion index (%)		11.3186	13.4871

TGA analysis

The TGA thermograms of these samples are shown in Fig. 6. It can be see from the profile of HA (Fig. 7a) that there is a little weight loss taken place upon heating, which indicates its thermal stability even at higher temperature. However, the observed weight loss at 25–100°C and 633.9°C could be ascribed to the loss of adsorbed water and decomposition of HPO_4^{2-} of n-HA, respectively. Figure 7b and c show the TG trace of KGM and CS, their thermal decomposition temperatures are at 280°C and 263°C, respectively. There are three steps of weight loss in the composite (Fig. 7d): the first weight loss is in the range of 25–98.3°C, which can be assigned to the loss of adsorbed water; the second at about 274.9°C can be attributed to the thermal decomposition of KGM-CS copolymer, and the third at 679.7°C may be due to decomposition of HPO_4^{2-} ion of n-HA. The obtained

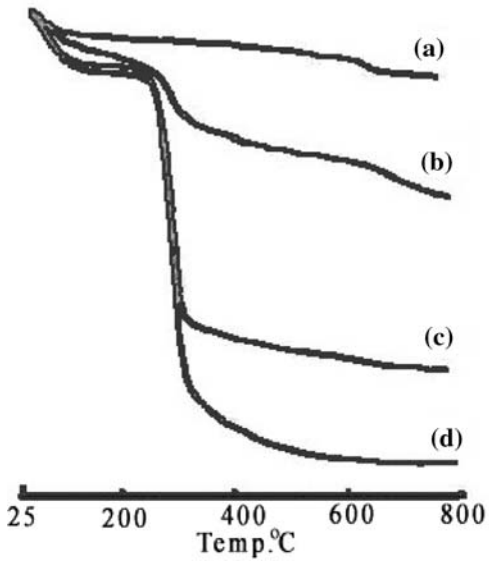

Fig. 7 TGA spectrum of n-HA (a), KGM (b), CS (c) and n-HA/KGM/CS composite (d)

results indicate that the incorporation of copolymer alters the thermal decomposition of n-HA matrix, which increases the second stage of decomposition. The total weight loss is found to be around 32 wt%. The content of organic phase is found to be almost identical with the initial addition during the reaction. So it is believed that KGM-CS copolymer is perfectly incorporated into the composite.

Interactive mechanism between n-HA and KGM-CS copolymer

When KGM and CS are blended, their molecule structures are disturbed. The mer units of polysaccharides, having some active groups, form three-dimensional networks. KGM forms stable interchains with CS after physical blended, which is due to that KGM has high molecular weight and characterizes the gel behavior. The van der Waals force is weak between KGM and CS, therefore, hydrogen bonding, hydrophilic interaction and electrostatic interaction play important roles in the interfacial formation. In the three kinds of molecular force, the hydrogen bonding is much more important than the other [20]. As for the two polymers, there may be existed plenty of hydrogen bonding in the chains. After physical blending, three-dimensional networks form in the KGM and CS by non-covalent bonding in the molecules. Biomolecules form non-Newtonian fluids due to the hydrogen bonding between n-HA and KGM-CS copolymer chains. KGM-CS copolymer includes net-in and net-tran forms [21]. According to TEM, XPS, IR, XRD and Rietveld analyses, it can be found that there has a stable interface formed between the three phases in the composite. The structure modes of composite mixture can be plotted as Fig. 8, based on Pang and Zhang and William P A's mode [20, 21].

The interactive bonding of molecules is shown in Fig. 9: there could be four different kinds of hydrogen bonding among the three phases in the composite. One is between O_6 and –NH in the blending process of the

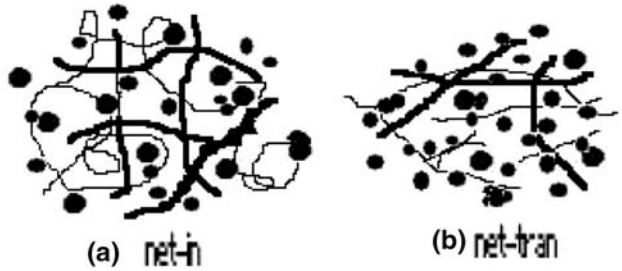

Fig. 8 Structure modes of composite mixture

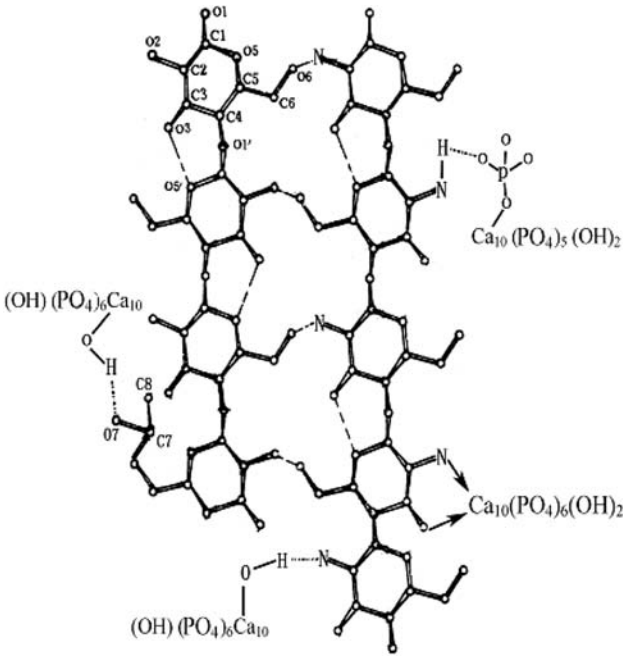

Fig. 9 Schematic of the kinds of bonding in composite

KGM-CS copolymer; the second is between OH^- and –C=O; the third is between –OH and –NH; the last one is between PO_4^{3-} and –NH. Besides, CS is characterized by forming CS-metal complexes in which metal ions coordinate with –NH groups of CS [22–25]. So coordinate bonding may happen between Ca^{2+} and –NH.

Conclusion

Hydrogen bonding has been formed between n-HA and KGM-CS copolymer in n-HA/KGM/CS composite and the hydrogen bonding mainly exists in four forms, i.e. O_6 and –NH; –OH and –C=O; –OH and –NH; PO_4^{3-} and –NH. Meanwhile, coordinate bonding may be formed between Ca^{2+} and –NH. Stable interfaces have been formed between the three phases in the composite.

This tri-phases composite material can be used as a degradable biomaterial for use of skeletal scaffold and tissue engineering, and so on.

Acknowledgements The author is appreciated the financial support of National 973 Key Basic Research Program (No.: 2004CB720604), and is also grateful for FT-IR data provided by Ms. Zhu Xiaohong (Analytical and Testing Center, Sichuan University), XRD data by Mr. Chen Shitu (Analytical and Testing Center, Sichuan University), and TGA data provided by Ms. Yang Zheng (Analytical and Testing Center, Sichuan University).

References

1. Jarcho M (1981) Clin Orthop Relat Res 157:259
2. Ogiso M (1998) J Biomed Mater Res Appl Biomater 43:318
3. Hench LL (1991) J Am Ceram Soc 74:1487
4. Bajpai PK (1992) In: Hulbert JA, Hulbert SF (eds) Bioceramics. Rose-Hulman Institute of Technology, Terra Haute, IN, p 87
5. Mi FL, Tan YC, Liang HF et al (2002) Biomaterials 23:181
6. David P, Manssur Y, Mark S (1992) Carbohydr Res 237:325
7. Tomihata K, Ikada Y (1997) Biomaterials 18:567
8. Muzzarilli RA (1993) Carbohydr Polym 20:7
9. Kato K, Matsuda K (1969) Agric Biol Chem 10:1446
10. Nutricol, Konjac General Technology Bulletin (1993) FMC Corporation. Food Ingredients Division, p 44
11. Ridout MJ, Brownsey GJ, Morris VJ (1998) Macromolecules 8:2539
12. Mi F-L, Tan Y-C, Liang H-F, Sung H-W (2002) Biomaterials 23:181
13. Qi Li, Li Guang-ji (2004) Polymer Bulletin 6:73
14. Rathje W (1939) Bodenk Pflernah 12:121
15. Larson AC, Von Dreele RB, Lujan M Jr (1990) GSAS-generalised crystal structure analysis system. Neutron Scattering Centre, Los Alamos National Laboratory, California, p 56
16. Jha LJ, Best SM, Knowles JC, Rehmna I, Santos JD (1997) J Mater Sci Mater Med 8:185
17. Bragg L (1919) The crystalline state. Vol (1) [M]. Bell G and Sons Ltds, London
18. Zhan Li, Yumin Du (2003) React Funct Polym 55:35
19. Ramaswamy V, Mccusker LB, Baerlocher CH (1999) Micropor Mesopor Mater 31:1
20. Pang Jie, Zhang Fu-sheng (2003) Polymer Mater Sci Eng 6:18
21. William PA, Philips GO (1995) Food Polysacch Appl 8:463
22. Ogawa K, Oka K (1993) Chem Mater 5:726
23. Inoue K, Baba Y, Yoshizuka K (1993) Bull Chem Soc Jpn 66:2915
24. Nishi N, Maekita Y, Nishimura S et al (1987) Int J Biol Macromol 9:109
25. Krajewska B (2001) React Funct Polym 47:37